A SET THEORETIC APPROACH TO TARGET DETECTION USING SPECTRAL SIGNATURE STATISTICS

David M. Rouse and H. Joel Trussell

Department of Electrical and Computer Engineering
North Carolina State University
Raleigh, NC 27695-7911

ABSTRACT

Pixels in hyperspectral images usually contain spectra from several classifiable objects, so that the recorded pixel is a mixture of the classes. Current methods estimate the proportion of each class using a set of spectral signatures describing only the class means. Since the means are known only by estimation methods, we introduce an approach that also incorporates the variation inherent in this estimation. The total least squares approach using projections onto convex sets (POCS) produces improved performance over simple maximum likelihood methods, even one that also uses the constraint sets and POCS.

1. INTRODUCTION

Due to spatial resolution limitations, images inevitably possess pixels comprising mixtures of spectrally distinct material classes. Such pixels may be described as a linear mixture of unique spectral signatures associated with the contents. The availability of hyperspectral imaging cameras has advanced the field of image classification using spectral signatures [1]. Each hyperspectral pixel contains spectral for data up to several hundred contiguous bands. With accurate estimates of the contributing spectral signatures, one may decompose pixels in terms of the proportion of each class material.

The first task is to obtain accurate estimates of the class spectral distributions (e.g. mean and covariance of the class spectral signature) found in the image under examination. Current methods determine estimates of only class spectral signature means. One method estimates the spectral signature means with the Optical Real-time Adaptive Spectral Identification System (ORASIS) [2]. This method autonomously establishes a set of spectral signatures from the image under investigation. Alternatively, a total least squares (TLS) estimate of spectral signature means from a set training samples of mixed pixels has been proposed [3].

Secondly, class proportion estimates with these spectral signature estimates have been obtained via quadratic programming (QP) [3] and orthogonal subspace projection (OSP) [4]. All of these methods neglect the variation in the spectral signature estimates and proceed to estimate the class proportions of a pixel only under the presence of measurement noise.

If it may be assumed *a priori* that an image contains certain spectral classes, estimates of the classes characterization have an error which must be taken into account. This error includes sampling errors as well as variations caused by different illuminations. Assuming measurement recording error on each pixel, the proportion estimates may be determined using TLS [5]. The proportionality estimate must be subject to certain constraints not supported by TLS, namely sum-to-one and nonnegativity. A weigthed TLS solution is implemented to accommodate the discrepancy between the variation associated with the pixel measurement noise and spectral distribution accuracy.

The set theoretic method of sequential projections onto convex sets (POCS) was shown to provide proportion estimates of discrete probability distributions contained in a discrete mixture distribution [6]. Similar sets describing the sum-to-one and nonnegativity constraints must be included to estimate a hyperspectral pixel's class proportions. For the problem of interest, the spectral data for a given pixel need not sum-to-one, but the proportions must sum-to-one.

This paper illustrates the use of the POCS method to classify objects and estimate mixtures in hyperspectral images using spectral distributions obtained *a priori* from histograms. As mentioned, this approach permits the implementation of the known solution characteristics: nonnegativity, summation constraints, and noise properties. Simulations provide evidence of the method's performance under various mixture proportions and the accuracy of the spectral distributions.

2. DESCRIPTION OF THE LINEAR MIXTURE MODEL

Let the column vector $\mathbf{r}_{L\times 1}$ represent the spectral data contained in a L band hyperspectral pixel. Assuming $K \leq L$

unique spectral classes, the contribution of each class is defined by the column vector $\mathbf{a}_{K\times 1}$. The linear mixture model is given by

$$\mathbf{r} = \mathbf{S}\mathbf{a} + \boldsymbol{\eta}, \tag{1}$$

where the k^{th} column of $\mathbf{S}$ represents the true spectral signature associated with the k^{th} class; the vector $\boldsymbol{\eta}$ models the measurement error, usually assumed to be independent and identically distributed (IID) from a zero mean, white noise random process with variance σ_η^2. However, the variability in a particular scene limits the precise knowledge of $\mathbf{S}$ for a given pixel $\mathbf{r}$. Thus, an estimate of the class spectral distributions must be formulated beforehand from a training set.

Let the estimate of the mean spectral signatures correspond to the columns of $\bar{\mathbf{S}}$ such that $\mathbf{S} = \bar{\mathbf{S}} + \Delta\mathbf{S}$. The perturbation matrix $\Delta\mathbf{S}$ is assumed to be an IID unbiased noise random process with variance σ_s^2. However, the true variance of the l^{th} band of the k^{th} spectral distribution is $\sigma_s^2(l,k)$. The linear mixture model in eq. (1) is more accurately written

$$\mathbf{r} = \left(\bar{\mathbf{S}} + \Delta\mathbf{S}\right)\mathbf{a} + \boldsymbol{\eta}. \tag{2}$$

The standard ML estimate does not support the additional noise described by $\Delta\mathbf{S}$. Note that the ML estimation method may provide adequate approximations of $\mathbf{a}$ by defining a column vector $\boldsymbol{\upsilon} = \Delta\mathbf{S}\mathbf{a} + \boldsymbol{\eta}$ containing all the noise sources present. The mixture model in eq. 2 is rewritten for ML estimation as

$$\mathbf{r} = \bar{\mathbf{S}}\mathbf{a} + \boldsymbol{\upsilon}. \tag{3}$$

Estimation methods designed to support the perturbation on the estimates of the mean spectral signatures $\bar{\mathbf{S}}$ and the measurement error associated with $\mathbf{r}$ include TLS and POCS. The common TLS solution assumes both perturbation sources possess the same variance [5]. This assumption would imply that the recording device and the spectral signature estimates have identical noise characteristics. A weighted TLS solution provides an estimate while recognizing this distinction in the noise variance. The method of POCS was shown to accommodate the weighted TLS method [7]. Additional known constraints on the model are welcomed by the POCS method. Sets need only be constructed to describe the constraints.

The nature of this mixture problem imposes constraints on $\mathbf{a}_{K\times 1}$. Since $\mathbf{a}$ represents proportions of the K classes in the recorded mixture, the elements of $\mathbf{a}$ must sum to one and lie on the interval $\left[0,1\right]$. The vector $\mathbf{a}$ is constrained to the set S_a defined in eq. (4).

$$S_a = \left\{ \mathbf{a} \in \Re^K \;\middle|\; \sum_{k=1}^{K} a_k = 1, \quad a_k \geq 0 \right\} \tag{4}$$

Set theoretic estimation with POCS is presented to solve the weighted TLS problem described by eq. (2) satisfying the additional constraints in eq. (4).

3. ESTIMATION METHOD

3.1. Set Theoretic Solution

Set theoretic estimation utilizes *a priori* knowledge about a signal to generate a feasible estimate [8]. Sets $\left\{S_i\right\}_{i=1}^{m}$ constructed with regard to known constraints of the signal possess an intersection containing the signal. A point in the intersection of all defined sets $S_0 = \bigcap_{i=1}^{m} S_m$ provides an estimate of the signal. Note that under these conditions a unique solution is not guaranteed. When all defined sets are closed and convex, an estimate may be found using POCS. The sets describing the known constraints are presented followed by a definition of their projector.

3.1.1. Noise Variance Set

For the noise constraint, the set with regard to the ML residual definition is modified since $\mathbf{S} = \bar{\mathbf{S}} + \Delta\mathbf{S}$. Applying the triangle inequality and the additional noise parameter σ_υ^2 modifies the ML residual set to

$$S_\eta = \left\{\mathbf{a} \;\middle|\; \left\|\mathbf{r} - \bar{\mathbf{S}}\mathbf{a}\right\|^2 \leq \sigma_\eta^2 + \sigma_\upsilon^2\right\}, \tag{5}$$

where $\sigma_\eta^2 = E\left\|\boldsymbol{\eta}\right\|^2$ and $\sigma_\upsilon^2 = E\left\|\Delta\mathbf{S}\mathbf{a}\right\|^2$. Alternatively, as shown in [7] the set S_η may be defined based on weighted total least squares (TLS) as

$$S_{TLS} = \left\{\mathbf{a} \;\middle|\; \exists\left\{\Delta\mathbf{S}, \boldsymbol{\eta}\right\} \ni \left(\bar{\mathbf{S}} + \Delta\mathbf{S}\right)\mathbf{a} = \mathbf{r} + \boldsymbol{\eta}, \right.$$
$$\left. \tau\left\|\Delta\mathbf{S}\right\|_F^2 + \left\|\boldsymbol{\eta}\right\|^2 \leq \nu\right\}, \tag{6}$$

where the parameters τ and ν are determined by statistical properties of $\Delta\mathbf{S}$ and $\boldsymbol{\eta}$. It was shown in [7] that S_{TLS} may also be defined by

$$S_{TLS} = \left\{\mathbf{a} \in \Re^N \;\middle|\; \left\|\bar{\mathbf{S}}\mathbf{a} - \mathbf{r}\right\|^2 - \frac{\nu}{\tau}\left\|\mathbf{a}\right\|^2 - \nu \leq 0\right\}, \tag{7}$$

where τ and ν are chosen to satisfy the following

$$\nu = \tau E\left\|\Delta\mathbf{S}\right\|_F^2 + E\left\|\eta\right\|^2 \qquad \tau \geq \frac{E\left\|\eta\right\|^2}{\sigma_K^2\left(\bar{\mathbf{S}}\right) - E\left\|\Delta\mathbf{S}\right\|_F^2}, \tag{8}$$

where $\sigma_K\left(\bar{\mathbf{S}}\right)$ denotes the smallest singular value of $\bar{\mathbf{S}}$.

3.1.2. Other Sets

The set S_a defined in eq. (4) is decomposed into two appropriate sets. The set S_Σ defines the summation to one constraint of the vector elements, and the set S_n defines the set of nonnegative vectors.

3.1.3. Projection onto Sets

The projection onto the set S_{TLS} is

$$\mathbf{a}_0 = \left[\mathbf{I} + \lambda_\eta \left(\bar{\mathbf{S}}^T\bar{\mathbf{S}} - \frac{\nu}{\tau}\mathbf{I}\right)\right]^{-1}\left(\hat{\mathbf{a}} + \lambda_\eta \bar{\mathbf{S}}^T\mathbf{r}\right), \qquad (9)$$

where $\hat{\mathbf{a}} \notin S_{TLS}$ and λ_η is the Lagrange multiplier satisfying $f(\mathbf{a}_0)$, where [7] defines $f(\cdot)$ as

$$f(\mathbf{a}) \equiv \left\|\bar{\mathbf{S}}\mathbf{a} - \mathbf{r}\right\|^2 - \frac{\nu}{\tau}\left\|\mathbf{a}\right\|^2 - \nu.$$

The projection onto the set S_Σ is

$$\mathbf{a}_0 = \hat{\mathbf{a}} - \frac{1}{K}\left(\hat{\mathbf{a}}^T\mathbf{1} - 1\right)\mathbf{1}_{K\times 1}, \qquad (10)$$

where $\hat{a} \notin S_\Sigma$.

The projection onto the nonnegativity set S_n is performed by replacing negative elements of $\hat{\mathbf{a}}$ with zeros to form $\mathbf{a}_0$.

4. SIMULATIONS

This section describes the simulations implemented to test the theory presented. A brief description of the formation of the mean spectral signatures is included. A one-dimensional simulated image is presented with an example image. Mean-squared error (MSE) statistics were obtained for each simulation. We compare the two POCS-based estimates with the classic ML estimate and use the ML estimate as the initial estimate for POCS. It is known that the initial estimate affects the outcome. The investigation of more effective initial estimates continues.

4.1. Formation of Sample Pixels

Four ($K = 4$) spectral classes, including a target, were defined for simulations of hyperspectral pixels from $L = 31$ band spectral data from the data set [9]. The four classes have $N_k = 100$ training examples to simulate illumination variants. Mean spectral signature estimates were formed from these basis signatures and are shown in Fig. 1. The noise power of $\Delta\mathbf{S}$ was estimated from the training set of N_k examples. The noise set defined in eq. (7) must satisfy $\sqrt{\frac{\nu}{\tau}} \leq \sigma_K$ to guarantee a convex set. This limits the estimate of the noise power of $\Delta\mathbf{S}$. The parameter τ was set at 10 times the value defined by eq. (8).

Random proportions of the basis signatures were mixed to simulate a class sample. A set of hyperspectral pixels was formed from random mixtures of the simulated class samples adhering to the constraint in eq. (4).

4.2. Target Proportion Simulation

A set of 21 hyperspectral pixels were constructed without contributions from the target class. Pixels 5, 10, 15, and 20 were modified to contain 20, 15, 10, and 5 percent of the target class, respectively. White Gaussian noise was added to each pixel to simulate a SNR of 30dB.

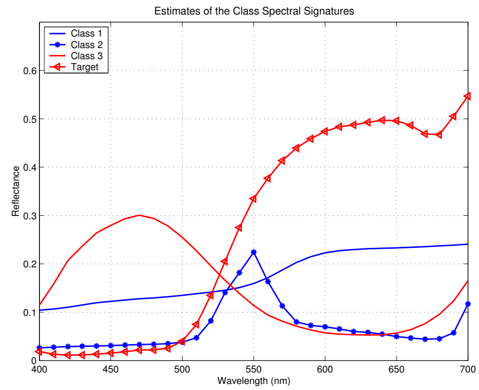

Fig. 1. Estimates of the Class Spectral Signatures

4.3. Hyperspectral Image Simulation

A 75×75 pixel image was generated containing pixels of pure class spectra. A square set of pixels containing sample target spectra was placed at a random location in the image. The simulated image is blurred with a PSF with dimensions 5×5 to mix adjacent pixels. Simulated recording noise in a capturing device with a SNR of 30dB is added as a zero mean Gaussian white noise process. Finally, the image was sub-sampled by saving every 5th pixel of the image. Fig. 2 shows the original image of pure class pixels (left) and the resulting image of mixed spectra (right).

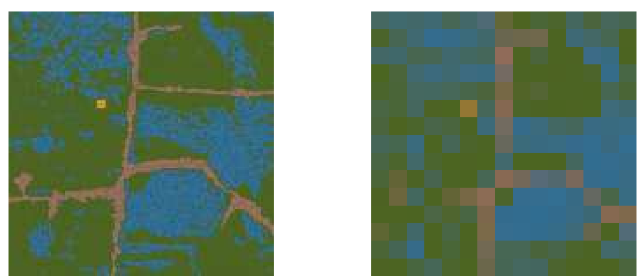

Pure Spectra [75 x 75]   Mixed Spectra [15 x 15]

Fig. 2. Hyperspectral Image

5. RESULTS

The first simulations illustrate the accuracy of the mean spectral signature. Figure 3 shows the target proportion estimates when the SNR of the estimates of the mean spectral signatures is 20dB. The POCS-ML estimate uses the noise set defined in eq. (5) with $\sigma_v^2 = 0$ and σ_η^2 as given for the simulation. The MSE of the estimated proportions of $\mathbf{a}$ overall and for the target proportion is given in Table 1.

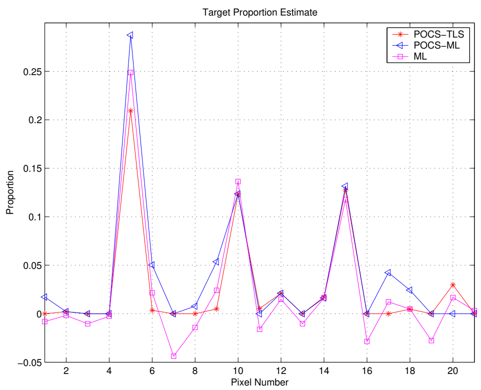

Fig. 3. Target Proportion Simulation Results with SNR of 20dB $\Delta\mathbf{S}$ and 30dB for σ_η^2, see Table 1

Table 1. MSE of Estimated $\mathbf{a}$ (dB)

	Overall	Target
ML	-19.85	-33.23
POCS-ML	-27.13	-30.06
POCS-TLS	-28.10	-38.76

The performance of the POCS-ML in comparison to the POCS-TLS method are under further investigation. The general ML estimate without the constraint given in eq. (4) clearly does not always provide feasible results. Both POCS estimates satisfy these constraints.

Simulations were also performed to illustrate mixed spectra due to blurring. Figure 4 shows the true (left) and POCS-TLS estimate (right) of the target proportion in each pixel. The scale was set as the minimum and maximum value of the image. The simulation illustrates the POCS-TLS estimate for a true target proportion of 0.36. The POCS-TLS method classified some other pixels as possible targets with much lower proportions, but the true target location is identified.

6. CONCLUSIONS

The POCS methods provide solutions that satisfy the sum-to-one and nonnegativity constraints on $\mathbf{a}$ and, thus, result in improvements over the classic ML estimate. The TLS approach by taking advantage of a more accurate model of system inaccuracies produces a slightly better estimate for this problem.

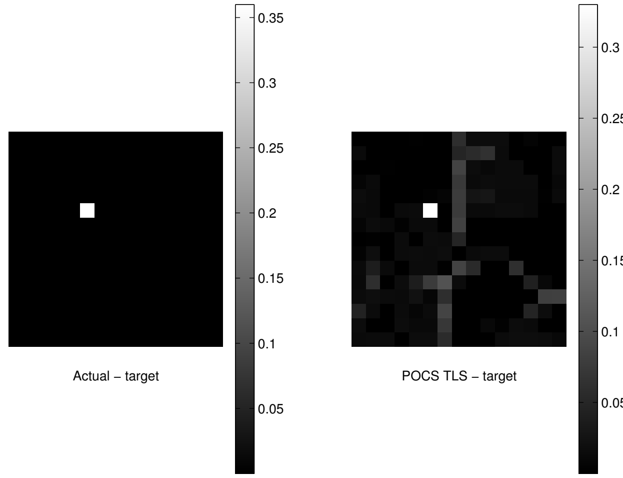

Fig. 4. Image Simulation Results (Target) with SNR of 20dB $\Delta\mathbf{S}$ and 30dB for σ_η^2

7. REFERENCES

[1] *IEEE Signal Processing Mag., Special Issue on Hyperspectral Imaging*, vol. 19, Jan. 2002.

[2] P. Palmadesso, J. Antoniades, M. Baumback, J. Bowles, and L. Rickard, "Use of filter vectors and fast convex set methods in hyperspectral analysis," in *Proceedings of the International Symposium on Spectral Sensing Research*, 1995.

[3] Y. H. Hu, H. B. Lee, and F. L. Scarpace, "Optimal linear spectral unmixing," *IEEE Trans. Geosci. Remote Sensing*, vol. 37, pp. 639–644, 1999.

[4] J. C. Harsanyi and C.-I. Chang, "Hyperspectral image classification and dimensionality reduction: An orthogonal subspace projection approach," *IEEE Trans. Geosci. Remote Sensing*, vol. 32, pp. 779–785, 1994.

[5] S. van Huffel and J. Vandewalle, *The Total Least Squares Problem*. Philadelphia, PA: SIAM, 1991.

[6] D. M. Rouse and H. J. Trussell, "Estimation of mixture densities from histograms," in *Proc. of IEEE ICASSP 2004*, Montreal, Canada, May 17-21, 2004.

[7] G. Sharma and H. J. Trussell, "Set theoretic signal restoration using and error in variables criterion," *IEEE Trans. Image Processing*, vol. 6, pp. 1692–1697, 1997.

[8] P. L. Combettes, "The foundations of set theoretic estimation," *Proc. IEEE*, vol. 81, pp. 182–208, 1993.

[9] M. Vrhel, R. Gershon, and L. Iwan, "Measurement and analysis of object reflectance spectra," *Color Research and Application*, vol. 19, no. 1, pp. 4–9, 1994.